Identification of a prognostic model using immune related genes combined with tumour mutational burden and T cell infiltration in triple-negative breast cancer

YOU MENG[1*], ZE-XIN HAN[2*], JIE ZHU[3*], YING WANG[4], YUE-QING HUANG[5], ZHONG-HUA ZOU[2], YU-YUAN MA[1], YI-FAN LI[6], HAN WANG[7], YING LI[2], LIAN LIAN[8] and WEN-JIE WANG[2]

[1]Department of Thyroid and Breast Surgery, Suzhou Municipal Hospital, The Affiliated Suzhou Hospital of Nanjing Medical University, Suzhou, Jiangsu 215001, P.R. China; [2]Department of Radio-oncology, Suzhou Municipal Hospital, The Affiliated Suzhou Hospital of Nanjing Medical University, Suzhou, Jiangsu 215001, P.R. China; [3]Department of Oncology, Changzhou Traditional Chinese Medicine Hospital, Changzhou, Jiangsu 213003, P.R. China; [4]Department of Oncology, Suzhou Municipal Hospital, The Affiliated Suzhou Hospital of Nanjing Medical University, Suzhou, Jiangsu 215001, P.R. China; [5]Department of Gastrointestinal Surgery II, Renmin Hospital of Wuhan University, Wuhan, Hubei 430060, P.R. China; [6]Department of Oncology, Binzhou People's Hospital, Binzhou, Shandong 256601, P.R. China; [7]Department of Oncology, Jining Cancer Hospital, Jining, Shandong 272004, P.R. China; [8]Department of Oncology, Suzhou Xiangcheng People's Hospital, Suzhou, Jiangsu 215131, P.R. China

Received April 29, 2025; Accepted December 22, 2025

DOI: 10.3892/ol.2026.15597

Abstract. Triple-negative breast cancer (TNBC) is one of the most aggressive molecular subtypes of breast cancer and immune-checkpoint blockade therapy has markedly changed the treatment landscape for this malignancy. Tumour-infiltrating lymphocytes (TILs) and tumour mutational burden (TMB) predict patient response to treatment with immune checkpoint inhibitors and reflect patient outcomes. The present study aimed to develop a TIL-based prognostic model, create a list of immune-related genes (IRGs) to inform clinicians of possible outcome predictions and generate a clinically relevant estimate of potential benefit from immunotherapy in TNBC. The present study included a cohort of 130 patients that were classified into two groups, namely $TMB^{high}/CD8^+$ T-cell-rich and $TMB^{low}/CD8^+$ T-cell-poor. Differential expression analysis using the 'edgeR' package identified IRGs associated with survival. The identified IRGs were included in a univariate Cox analysis to derive a prognostic signature. In addition, the present study examined how the signature genes were associated with immune cell infiltration using the Tumour IMmune Estimation Resource database. The final four-gene signature, C-X-C motif chemokine ligand 13 (CXCL13), latent TGF-β binding protein 2, placental growth factor and transporter associated with antigen processing binding protein-like (TAPBPL), stratified risk robustly: Patients in the high-risk group had significantly worse overall survival compared with low-risk patients in both prognostic and validation models. Compared with high-risk patients, low-risk patients had greater infiltration of $CD8^+$ T cells, M1 macrophages, resting dendritic cells and activated $CD4^+$ T cells and less infiltration of both M0 and M2 macrophages. Higher CXCL13 and TAPBPL expression levels were significantly associated with higher $CD8^+$ T-cell counts and inversely associated with M0 and M2 macrophage counts. The overall risk score and CXCL13 expressions were all positively correlated with multiple immune checkpoint genes, while TAPBPL expression correlated positively with CTLA4, TIM3 and TIGIT. In summary, the present study provided a TMB- and T-cell infiltration-based IRG signature that is prognostic and may potentially support the prediction of immunotherapy responsiveness in TNBC in the future.

Correspondence to: Dr Wen-Jie Wang, Department of Radio-oncology, Suzhou Municipal Hospital, The Affiliated Suzhou Hospital of Nanjing Medical University, 16 Baita West Road, Suzhou, Jiangsu 215001, P.R. China
E-mail: suda_wangwenjie@163.com

Dr Lian Lian, Department of Oncology, Suzhou Xiangcheng People's Hospital, 1060 Zhenghuayuan Road, Suzhou, Jiangsu 215131, P.R. China
E-mail: dr_lianlian@163.com

*Contributed equally

Key words: C-X-C motif chemokine ligand 13, immune-related gene, immune cell infiltration transporter associated with antigen processing binding protein-like, triple-negative breast cancer

Introduction

With estimated 2.3 million new cases and 670,000 deaths globally, breast cancer accounted for ~25% of new female cancer diagnoses and 15.5% of cancer-related mortality in 2022 (1). Breast cancer is classified histopathologically and molecularly into luminal A/B, HER-2-enriched and triple negative breast cancer (TNBC). TNBC accounts for 10-20% of global breast cancer cases (2). TNBC is characterised by a poor prognosis

that is associated with its aggressive behaviour, intrinsic chemoresistance and tendency to early relapse/metastatic spread (3). Further molecular sub-stratification has separated TNBC into basal-like, immunomodulatory, mesenchymal, mesenchymal stem-like and luminal androgen receptor (4). TNBC exhibits higher immunogenicity compared with other subtypes, characterized by increased tumour-infiltrating lymphocytes (TILs), programmed death-ligand 1 (PD-L1) expression and tumour mutational burden (TMB) (5). Key immune-related genes (IRGs) influencing prognosis and response to immunotherapy include programmed cell death protein 1 (PD-1), PD-L1, cytotoxic T-lymphocyte-associated protein 4 (CTLA4), and genes involved in antigen presentation (human leukocyte antigen), cytokine signalling [interferon-γ (IFNG) and CXCL chemokines] and T-cell function (granzyme B and perforin-1), highlighting potential therapeutic targets (6).

Treatment strategies for breast cancer have made certain notable advancements in the past two decades. Fibroblast growth factor receptor 4 promotes TNBC progression by activating the AKT/ryanodine receptor type 2 axis, reprogramming fatty acid metabolism (7). Separately, circXPO6 stabilizes c-Myc to enhance glycolysis (glucose transporter type 1/hexokinase 2/monocarboxylate transporter 4), driving tumour growth (8). Both pathways are associated with poor prognosis and offer therapeutic targets. However, for patients with metastatic TNBC, immune-checkpoint blockade, particularly targeting PD-1/PD-L1, demonstrated promising results (9).

TILs are key effectors and regulatory factors of the tumour microenvironment and they have been closely associated with clinical outcomes in patients with breast cancer, particularly those achieving complete pathological response after neoadjuvant chemotherapy (10,11). In TNBC, increased TIL density is associated with chemosensitivity and lower likelihood of recurrence (12,13). While $CD8^+$ cytotoxic T cells comprise one component, one of the strongest relationships with survival in breast cancer cohorts is the frequency of $CD8^+$ TILs (14). TIL levels can also predict sensitivity to immune-checkpoint inhibitors (ICIs): PD-1 expression is frequently high in the presence of rich lymphocyte infiltration, which enhances therapeutic response benefit (15-17).

TMB is defined as the number of somatic sequence variants per megabase of tumour DNA. A higher TMB should create neo-antigens that sharpen immune recognition, increase sensitivity to immune-checkpoint blockade and provide improved response rates and survival (18-20). As with TILs, TMB is an accepted biological marker in predicting the effectiveness of ICIs (21,22). Assessments of transcriptomic data on a large scale also suggest that groups of co-expressed genes predict the number and function of TILs and are prognostic markers (23-25). Recently, ICIs have exhibited promising activity in TNBC treatment (26,27). Furthermore, previous studies (28,29) have demonstrated that high TMB is notably associated with enhanced T cell infiltration, improved response to ICIs and prolonged survival in TNBC. Considering the prognostic role of TMB and TILs in cancer outcome and immunotherapy response, the present study chose TMB and TILs as the entry point (28,30).

Despite progress in therapies and prognostic markers, the majority of patients with TNBC still have a poor outcome. Therefore, the present study aimed to identify differentially expressed IRGs (DEIRGs), associating with survival, by using a combination of TMB and the density of $CD8^+$ T lymphocytes; ii) develop a personalised, TIL-based prognostic model; iii) create a list of IRGs to inform clinicians of possible outcome predictions; and iv) generate a clinically relevant estimate of potential benefit from immunotherapy in TNBC.

Material and methods

Data acquisition and processing. RNA-sequencing data and clinical details for TNBC were downloaded from The Cancer Genome Atlas (TCGA; https://portal.gdc.cancer.gov/) database. After quality control (selecting 'RNA-sequence', 'prognosis' and 'TNBC' in TCGA database), 130 cases (age range, 26-90 years; all female) were evaluated. Tumours were stratified according to the median values for both TMB and $CD8^+$ T-cell infiltration into $TMB^{high}/CD8^{high}$ and $TMB^{low}/CD8^{low}$. The baseline characteristics are shown in Table I. IRGs from the Immunology Database and Analysis Portal (ImmPort) database (https://immport.niaid.nih.gov/home) were used for the present analysis (31). For external validation, the expression profiles from 107 TNBC samples in the Gene Expression Omnibus (GEO) database (GSE58812) were analysed (ncbi.nlm.nih.gov/geo/query/acc.cgi?acc=GSE58812 (32).

Identification of differentially expressed genes (DEGs), DEIRGs and survival-associated DEIRGs. The 'edgeR' package (http://bioconductor.org/packages/edgeR/) in R software (R Development Core Team, version 4.2.2) was applied to screen out DEGs. Statistical significance was defined based on criteria such as $\log_2$ (fold-change) >0.5 and a false-discovery rate-adjusted P<0.05 (33). Volcano plots and heatmaps were produced using the 'gplots' (cran.r-project.org/web/packages/gplots/) and 'heatmap' (stat.ethz.ch/R-manual/R-devel/library/stats/html/heatmap.html) functions. By mapping the significant genes in the ImmPort catalogue, DEIRGs were derived. Univariate Cox proportional-hazards modelling was used to identify DEIRGs which were associated with overall survival (OS) and cross-validated in the GSE58812 dataset.

Building the immune-related gene prognostic index (IRGPI). Survival-associated IRGs were refined using the least absolute shrinkage and selection operator-penalized Cox regression and transformed into a composite risk score. Patients from the GSE58812 dataset were split into high- and low-risk groups according to the median IRGPI and Kaplan-Meier curves were used to compare survival between strata. The risk-score formula was calculated as follows (34):

$$\text{SurvivalRiskScore (SRS)} = \sum_{i=1}^{k} (C_i \times V_i)$$

In the formula, 'k' represents the number of prognostic indicators involved in the model, 'C_i' represents the coefficient of the prognostic indicators in multivariate Cox regression

Table I. Clinical features of patients with TNBC in TCGA.

Clinical features	Patients (n=130), n (%)
Median age (range), years	53 (26-90)
T stage	
T1	33 (25.38)
T2	82 (63.08)
T3	11 (8.46)
T4	4 (3.08)
N stage	
0	87 (66.92)
1	28 (21.54)
2	10 (7.69)
3	5 (3.85)
G3	39 (30.00)
AJCC stage	
1	22 (16.92)
2	87 (66.92)
3	21 (16.16)

AJCC, American Joint Committee on Cancer; G3, poorly differentiated (high grade); N, lymph node; T, tumour; TCGA, The Cancer Genome Atlas; TNBC, triple-negative breast cancer.

analysis and 'V_i' represents the specific value of the prognostic indicator.

Relationship between survival-associated IRGs and immune cell infiltration. Using the Tumour IMmune Estimation Resource (TIMER) database (cistrome.shinyapps.io/timer/) (35), the infiltration landscape of immune cells in tumour-resident immune cells was investigated. The TIMER repository consists of 10,897 TCGA samples across 15 tumour types and quantifies the densities of eight immune subsets [B cells, $CD4^+$ and $CD8^+$ T cells, natural-killer (NK) cells, regulatory T cells (Tregs), macrophages, dendritic cells (DCs) and monocytes]. For each patient with TNBC, the infiltration values were derived and correlated with the IRGPI.

Relationship between the immune prognostic model and clinical characteristics and outcome. The present study evaluated whether the IRGPI offered prognostic value over standard variables by performing both univariate and multivariate Cox regression for age, American Joint Committee on Cancer (AJCC) stage and tumour (T) and lymph node (N) status (36).

Tumour dysfunction and exclusion (TIDE) score analysis. Potential for immune-escape was assessed using TIDE analysis (tide.dfci.harvard.edu/login), which integrates T-cell dysfunction and exclusion markers to predict the response to checkpoint blockade.

Immunohistochemistry (IHC). TNBC tissues collected from 10 female patients at Suzhou Municipal Hospital from June 2016 to May 2018 (Suzhou, China; aged 30-78 years; median age of 53 years; initial diagnosis of TNBC in post-operative or puncture specimens; not received any treatment and provided written informed consent) were fixed for 24 h in 4% paraformaldehyde/PBS and at 4˚C. The tissues were sliced into 3-5 μm-thick sections. The slides were treated with 0.3% H_2O_2/PBS at room temperature for 10 min to eliminate endogenous peroxidase activity. The slides were treated with 5% goat serum (cat. no. 16210064; Thermo Fisher Scientific, Inc.) for 30 min at room temperature. The slides were further stained for CD8, C-X-C motif chemokine ligand 13 (CXCL13), TAP binding protein like (TAPBPL), latent TGF-β binding protein 2 (LTBP2) and placental growth factor (PGF). TNBC tissues were incubated overnight at 4˚C with primary antibodies against CD8 (1:1,000; cat. no. GB12068; Wuhan Servicebio Technology Co., Ltd.), CXCL13 (1:1,000; cat. no. GB11919; Wuhan Servicebio Technology Co., Ltd.), TAPBPL (1:200; cat. no. 201030-T08; Sino Biological, Inc.), LTBP2 (1:200; cat. no. OACD05363; Beijing Aovia Biotechnology Co., Ltd.) and PGF (1:500; cat. no. 10642-1-AP; Proteintech Group, Inc.), which was followed by incubation with HRP-conjugated secondary antibodies (goat anti-rabbit IgG, 1:1,000; cat. no. G1301; Wuhan Servicebio Technology Co., Ltd.) at room temperature for 30 min. Tissue sections were stained with 3,3'-diaminobenzidine at room temperature for 10 min, counterstained with haematoxylin at room temperature for 15 min, dehydrated using a series of ethanol and then mounted. Two pathologists, blinded to clinical information, scored staining intensity using the histochemistry Score) semi-quantitative system by light microscope (Olympus CX33 Corporation) (37).

Statistical analysis. Survival curves were generated using the 'survival' R package and differences were assessed using the log-rank test. Time-dependent areas under the curves were generated using the 'survivalROC' package (v1.0.3, cran.r-project.org/web/packages/survivalROC/index.html). A two-sided $P<0.05$ was considered to indicate a statistically significant difference. The present study conducted association analyses of the risk score, CXCL13, TAPBPL, PGF and LTBP2 with immune cell infiltration separately, employing the unpaired t-test, Mann-Whitney U test and Pearson's correlation analysis. Each independent experiment was repeated three times, and normality test was conducted using the Kolmogorov-Smirnov test. Data are presented as the mean.

Results

Patients in the $TMB^{low}/CD8^{low}$ group exhibited worse outcomes. By using median values as cut-offs, there was no significant survival difference between the TMB^{high} and TMB^{low} (Fig. 1A), and between the $CD8^{high}$ and $CD8^{low}$ cohorts (Fig. 1B). Patients classified as $TMB^{low}/CD8^{low}$ were associated with significantly worse OS compared with the $TMB^{high}/CD8^{high}$ cohort (Fig. 1C).

Identification of DEIRGs. A total of 225 immune genes with altered expression were identified using 'edgeR', with 88 IRGs identified as being upregulated and 137 IRGs identified as being downregulated (Fig. S1).

Table II. Univariate Cox regression analysis of TCGA and GEO databases.

	Overall survival			
	TCGA		GEO	
Gene	OR (95% CI)	P-value	OR (95% CI)	P-value
CXCL13	0.352 (0.122-0.979)	0.047[a]	0.253 (0.108-0.593)	0.002[b]
CXCL10	0.328 (0.114-0.949)	0.040[a]	0.434 (0.201-0.934)	0.033[a]
TAPBPL	0.191 (0.054-0.678)	0.010[a]	0.426 (0.194-0.937)	0.034[a]
IDO1	0.334 (0.116-0.965)	0.043[a]	0.356 (0.162-0.783)	0.010[a]
IFNG	0.265 (0.085-0.827)	0.022[a]	0.390 (0.177-0.857)	0.019[a]
APOBEC3C	0.304 (0.098-0.944)	0.039[a]	0.509 (0.240-1.078)	0.078
CCL5	0.339 (0.118-0.978)	0.045[a]	0.519 (0.245-1.100)	0.087
CCL13	0.150 (0.034-0.978)	0.013[a]	0.537 (0.254-1.139)	0.105
FABP7	0.284 (0.090-0.896)	0.032[a]	1.485 (0.709-3.110)	0.294
FOS	3.514 (1.107-11.151)	0.033[a]	1.339 (0.644-2.784)	0.434
LTBP2	3.328 (1.041-10.644)	0.043[a]	0.821 (0.395-1.706)	0.597
PDCD1	0.283 (0.091-0.879)	0.029[a]	0.353 (0.707-1.470)	0.353
PGF	3.361 (1.080-10.460)	0.036[a]	1.285 (0.618-2.672)	0.502
PSME1	0.192 (0.054-0.673)	0.010[a]	0.629 (0.300-1.318)	0.219

[a]P<0.05; [b]P<0.01. OR, odds ratio; TCGA, The Cancer Genome Atlas; GEO, Gene Expression Omnibus; CXCL, C-X-C chemokine motif ligand; TAPBPL, transporter associated with antigen processing binding protein-like; IDO1, indoleamine 2,3-dioxygenase 1; IFNG, interferon-γ; APOBEC3C, apolipoprotein B mRNA editing enzyme catalytic subunit 3C; CCL, C-C motif chemokine ligand; FABP7, fatty acid binding protein 7; FOS, Fos proto-oncogene, AP-1 transcription factor subunit; LTBP2, latent TGF-β binding protein 2; PDCD1, programmed cell death protein 1; PGF, placental growth factor; PSME1, proteasome activator subunit 1.

Screening for prognosis-related genes. Out of a total of 63 IRGs, univariate Cox analysis was performed on 14 IRGs that were significantly associated with survival in TCGA dataset (Table II).

Low risk-score group demonstrates improved OS in both prognostic and validation model. In TCGA prognostic model, the low risk-score group had improved OS compared with the high risk-score group (Fig. S2A; OS limited to 20 years). In the validation model, the high-risk group had worse OS compared with the low-risk score group (Fig. S2B). The formula of risk score was as follows: (Expression level of CXCL13 x-0.009833) + (expression level of TAPBPL x -0.016158) + (expression level of LTBP2 x 0.016080) + (expression level of PGF x 0.096733). The present study separated patients with TNBC into two groups (high- and low-risk score groups) with median risk score in TCGA model (Fig. S3A, C and E). The prognostic model was verified by a validation prognostic model based on the GEO database (Fig. S3B, D and F). Patients with a lower T stage (T1-2) had a significantly lower risk score compared with patients with stage T3-4 (Fig. S4).

Univariate and multivariate Cox regression analysis of prognostic model. Using univariate Cox regression analysis, advanced T stage [hazard ratio (HR)=4.384; 95% CI, 1.388-13.850], N Stage (HR=3.543; 95% CI, 1.282-9.794), AJCC stage (HR=7.210; 95% CI, 2.586-20.104) and risk score (HR=6.302; 95% CI, 1.786-22.235) were associated with an unfavourable prognosis (Table III). Multivariate analysis determined that the risk score was an independent prognostic factor for overall survival (HR=4.944; 95 % CI, 1.323-18.479; Table III).

Validation of the accuracy of the prognostic model. To substantiate the model, a nomogram was established from the multivariate Cox model that could compare predictive performance across age, AJCC, T and N stages and risk score. The receiver-operating characteristic curves shown in Fig. S5A demonstrated improved discrimination for the composite model. The nomogram, which included the five variables outlined earlier, generated a point value for each variable and higher total scores indicated lower 3-, 5- and 10-year survival probabilities (Fig. S5B).

Analysis of risk score and immune cell infiltration. Individuals classified into the low-risk cohort had a significantly higher immune score (IS; Fig. 2A). However, TMB values were not statistically different between high- and low-risk groups (Fig. 2B). Low-risk patients also had significantly higher $CD8^+$ T lymphocyte infiltration (Fig. 2C), M1 macrophages (Fig. 2F), resting DCs (Fig. 2M) and activated $CD4^+$ T lymphocytes (Fig. 2L), while both M0 (Fig. 2E) and M2 (Fig. 2G) macrophage densities were significantly lower (both P<0.001). Tregs (Fig. 2D), resting NK cells (Fig. 2H), risk score (Fig. 2I), naïve B lymphocytes (Fig. 2J), resting $CD4^+$ T cells (Fig. 2K), activated DCs (Fig. 2N) and monocytes (Fig. 2O) infiltration did not differ between risk groups.

Table III. Univariate and multivariate Cox regression analysis of TCGA prognostic model.

	Overall survival			
	Univariate		Multivariate	
Clinical feature	OR (95% CI)	P-value	OR (95% CI)	P-value
Age	0.517 (0.179-1.494)	0.223	-	-
T stage	4.384 (1.388-13.850)	0.012[a]	0.917 (0.218-3.851)	0.562
N stage	3.543 (1.282-9.794)	0.015[a]	2.135 (0.612-7.450)	0.234
AJCC stage	7.210 (2.586-20.104)	<0.01[a]	3.015 (0.690-13.176)	0.142
Risk score	6.302 (1.786-22.235)	0.004[a]	4.944 (1.323-18.479)	0.018[a]

[a]P<0.05. AJCC, American Joint Committee on Cancer; N, lymph node; T, tumour; TCGA, The Cancer Genome Atlas; TNBC, triple-negative breast cancer; OR, odds ratio.

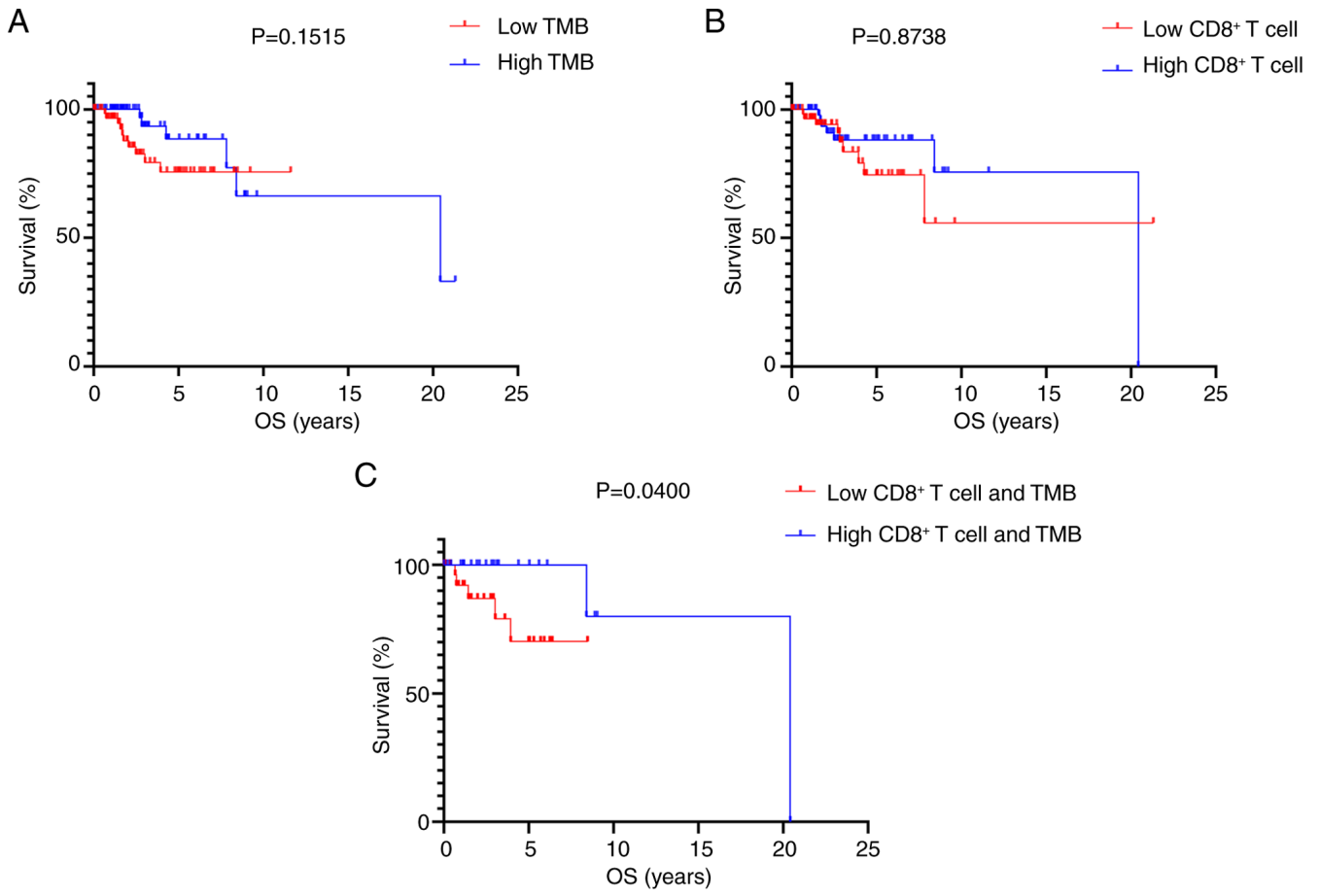

Figure 1. Prognostic relevance of CD8+ T cells and TMB in patients with TNBC. (A) TMB^{high} and TMB^{low} groups; (B) CD8+ T cell^{high} and CD8+ T cell^{low} groups; (C) TMB^{high}/CD8+ T cell^{high} and TMB^{low}/CD8+ T cell^{low} groups. TMB, tumour mutation burden; TNBC, triple-negative breast cancer; OS, overall survival.

Higher transcription levels of CXCL13 were accompanied by significantly higher IS (Fig. 3A) but were not associated with TMB (Fig. 3B). Samples with high CXCL13 levels had significantly greater recruitments of CD8+ T cells (Fig. 3C), activated CD4+ T cells (Fig. 3L) and M1 macrophages (Fig. 3F) and significantly lower levels of M0 (Fig. 3E) and M2 macrophages compared with those with low CXCL13 levels (Fig. 3G). Treg cells (Fig. 3D), resting NK cells (Fig. 3H), risk score (Fig. 3I), naïve B cells (Fig. 3J), resting CD4+ T cells (Fig. 3K), resting DCs (Fig. 3M), activated DCs (Fig. 3N) and monocytes (Fig. 3O) concentrations did not appear to be impacted by the level of CXCL13.

Similarly, enhanced levels of TAPBPL were significantly associated with higher IS (Fig. 4A) and not associated with

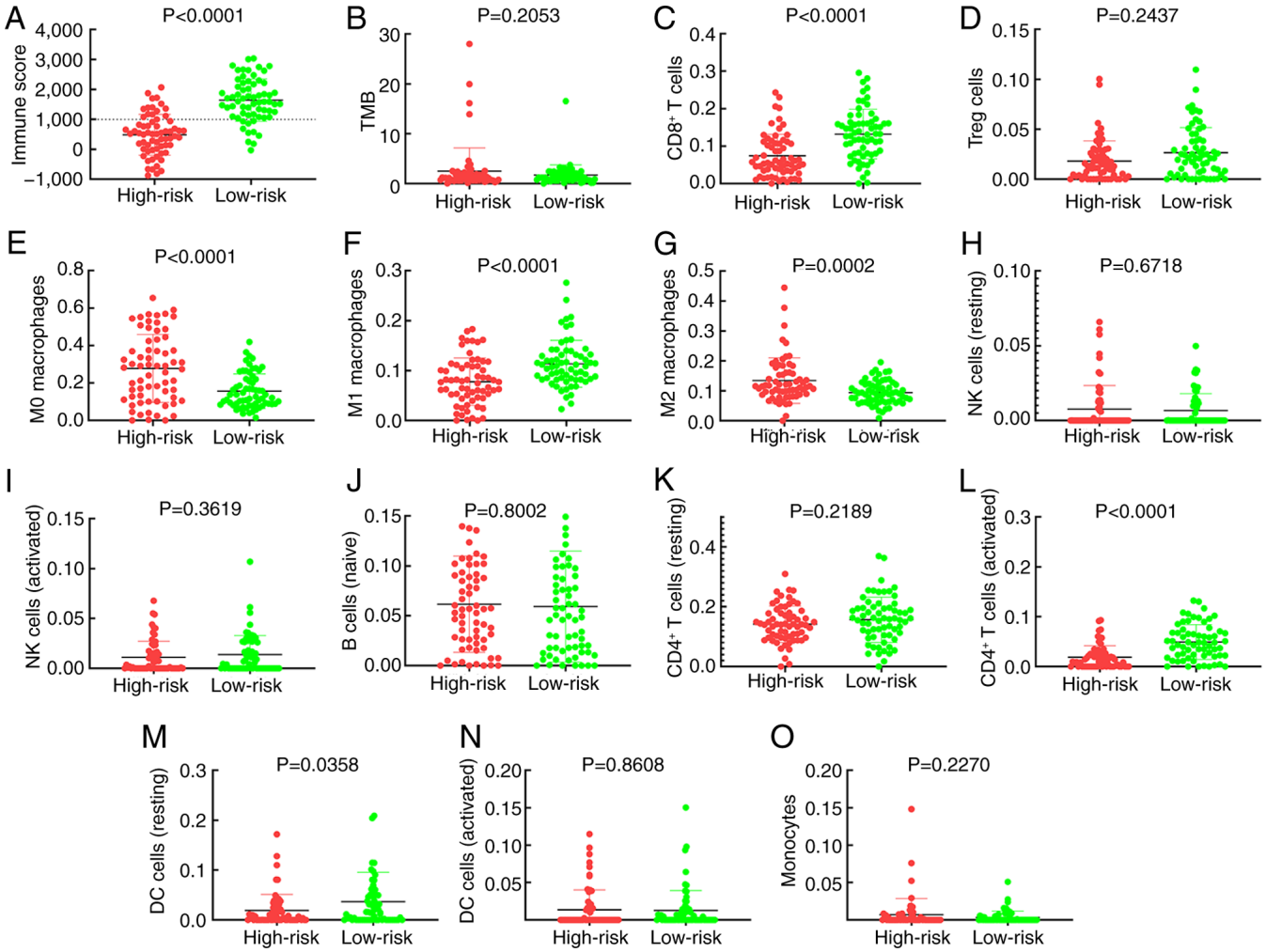

Figure 2. Risk score and immune cell infiltration association analysis using Mann-Whitney U test. Association of high- and low-risk groups with (A) immune score, (B) TMB, (C) $CD8^+$ T cells, (D) Treg cells, (E) M0 macrophages, (F) M1 macrophages, (G) M2 macrophages, (H) NK cells (resting), (I) NK cells (activated), (J) B cells, (K) $CD4^+$ T cells (resting), (L) $CD4^+$ T cells (activated), (M) DC cells (resting), (N) DCs (activated) and (O) monocytes. TMB, tumour mutation burden; Treg, regulatory T cell; NK, natural killer; DC, dendritic cell.

TMB (Fig. 4B). Increased levels of TAPBPL transcripts were significantly associated with greater infiltration of $CD8^+$ T lymphocytes (Fig. 4C) and with lower proportions of M0 (Fig. 4E) and M2 (Fig. 4G) macrophages. Treg cells (Fig. 4D), M1 macrophages (Fig. 4F), resting NK cells (Fig. 4H), risk score (Fig. 4I), naïve B cells (Fig. 4J), resting $CD4^+$ T cells (Fig. 4K), activated $CD4^+$ T cells (Fig. 4L), resting DCs (Fig. 4M), activated DCs (Fig. 4N) and monocytes (Fig. 4O) concentrations were not affected by whether TAPBPL was expressed.

Increased PGF expression, by contrast, was significantly associated with greater infiltration of M0 (Fig. 5E) and lower infiltration of M1 macrophages (Fig. 5F). PGF levels were not associated with IS (Fig. 5A) or TMB (Fig. 5B). PGF expression was also not associated with $CD8^+$ T cells (Fig. 5C), Treg cells (Fig. 5D), M2 macrophages (Fig. 5G), resting NK cells (Fig. 5H), risk score (Fig. 5I), naïve B cells (Fig. 5J), resting $CD4^+$ T cells (Fig. 5K), activated $CD4^+$ T cells (Fig. 5L), resting DCs (Fig. 5M), activated DCs (Fig. 5N) and monocytes (Fig. 5O) as well.

Increased LTBP2 expression was significantly associated with greater infiltration of resting $CD4^+$ T lymphocytes (Fig. 6K) and independent of IS (Fig. 6A) and TMB (Fig. 6B). LTBP2 levels did not influence infiltration of $CD8^+$ T lymphocytes (Fig. 6C), Treg cells (Fig. 6D), M0 macrophages (Fig. 6E), M1 macrophages (Fig. 6F), M2 macrophages (Fig. 6G), resting NK cells (Fig. 6H), risk score (Fig. 6I), naïve B cells (Fig. 6J), activated $CD4^+$ T cells (Fig. 6L), resting DCs (Fig. 6M), activated DCs (Fig. 6N) or monocytes (Fig. 6O).

Immune checkpoint-related genes correlation analysis. The composite risk score indicated a positive correlation with immune-checkpoint genes PD-L1, T-cell immunoglobulin and cytotoxic T-lymphocyte antigen 4 (CTLA-4) and TIGIT, but negatively with lymphocyte activation gene 3 (LAG3) (Fig.7). CXCL13 levels were also positively correlated with each of these immune-checkpoint genes (Fig. 8). TAPBPL levels correlated positively with mucin domain-containing protein 3 (TIM3), CTLA-4 and TIGIT, negatively with LAG3, (Fig. 9). PGF levels were not significantly correlated with PD-L1, TIM3, LAG3, CTLA-4 or TIGIT transcript levels either (Fig. 10). Lastly, LTBP2 levels correlated negatively with LAG3 levels, while no

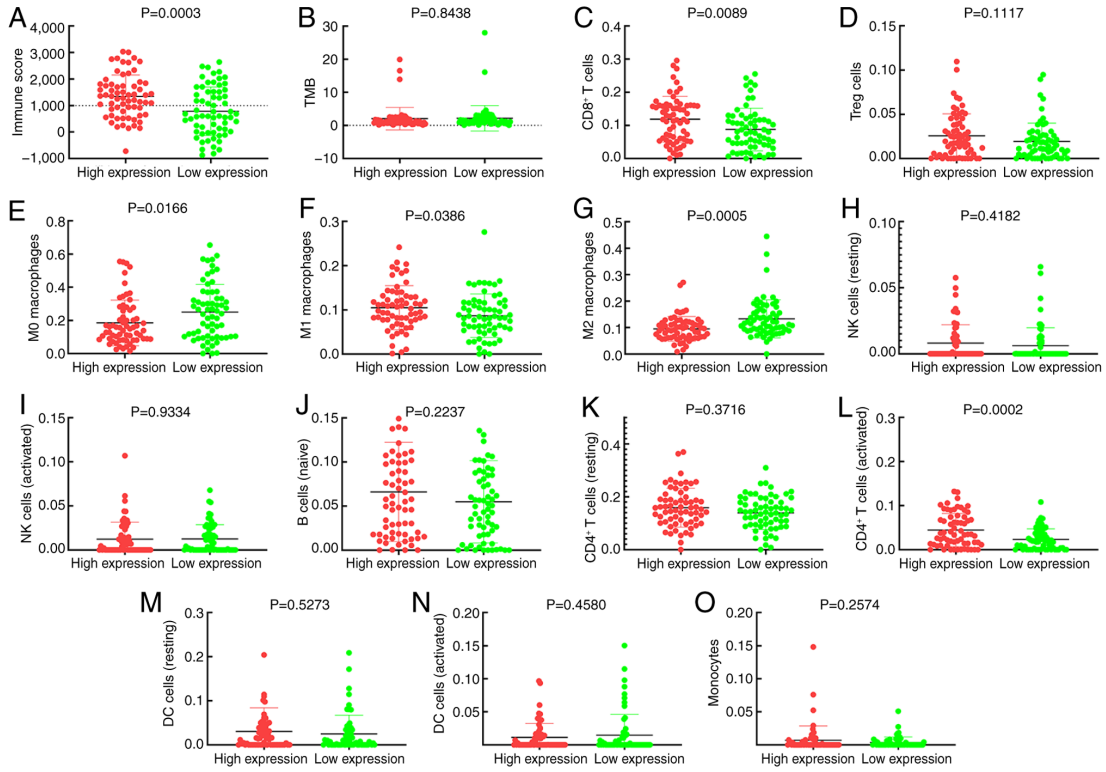

Figure 3. CXCL13 and immune cell infiltration association analysis using Mann-Whitney U test. Association of CXCL13 expression with (A) immune score, (B) TMB, (C) CD8+ T cells, (D) Treg cells, (E) M0 macrophages, (F) M1 macrophages, (G) M2 macrophages, (H) NK cells (resting), (I) NK cells (activated), (J) B cells, (K) CD4+ T cells (resting), (L) CD4+ T cells (activated), (M) DC cells (resting), (N) DCs (activated) and (O) monocytes. CXCL13, C-X-C motif chemokine ligand 13; TMB, tumour mutation burden; Treg, regulatory T cells; NK, natural killer; DC, dendritic cell.

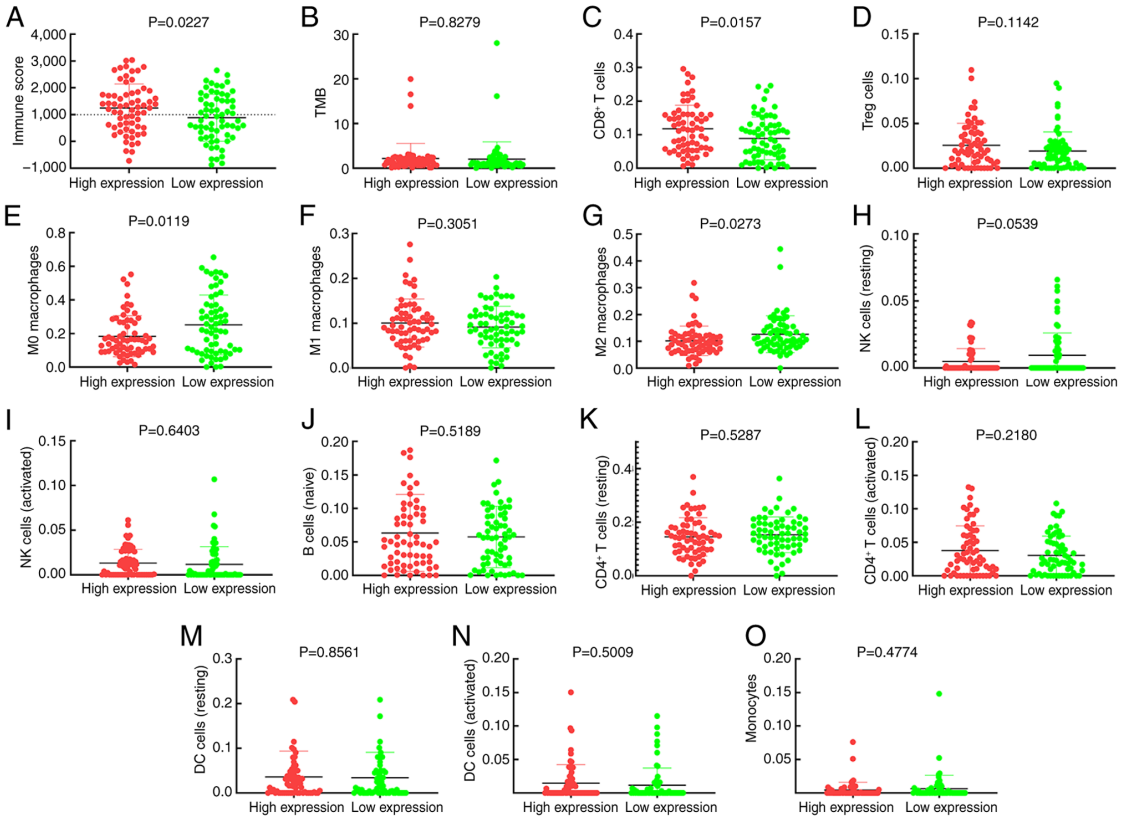

Figure 4. TAPBPL and immune cell infiltration association analysis by Mann-Whitney U test. Association of TAPBPL expression with (A) immune score, (B) TMB, (C) CD8+ T cells, (D) Treg cells, (E) M0 macrophages, (F) M1 macrophages, (G) M2 macrophages, (H) NK cells (resting), (I) NK cells (activated), (J) B cells, (K) CD4+ T cells (resting), (L) CD4+ T cells (activated), (M) DC cells (resting), (N) DCs (activated) and (O) monocytes. TAPBPL, transporter associated with antigen processing binding protein like; TMB, tumour mutation burden; Treg, regulatory T cells; NK, natural killer; DC, dendritic cell.

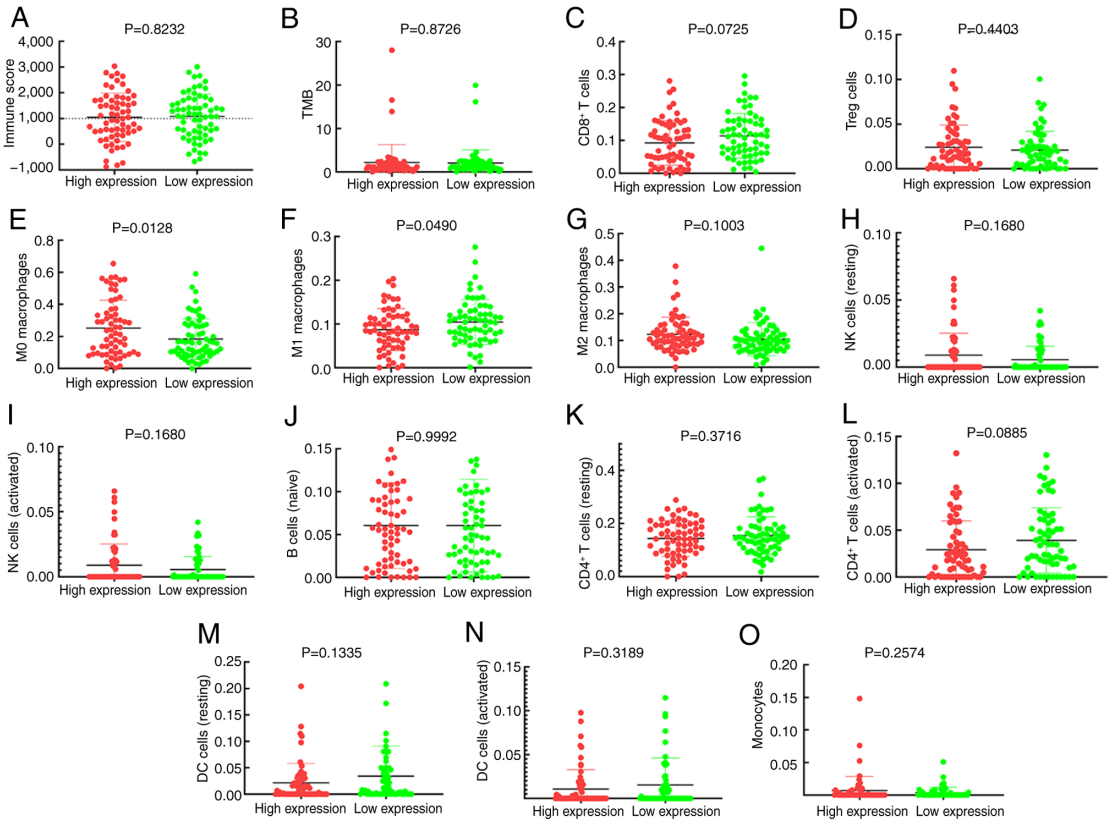

Figure 5. PGF and immune cell infiltration association analysis by Mann-Whitney U test. Association of PGF expression with (A) immune score, (B) TMB, (C) $CD8^+$ T cells, (D) Treg cells, (E) M0 macrophages, (F) M1 macrophages, (G) M2 macrophages, (H) NK cells (resting), (I) NK cells (activated), (J) B cells, (K) $CD4^+$ T cells (resting), (L) $CD4^+$ T cells (activated), (M) DC cells (resting), (N) DCs (activated) and (O) monocytes. PGF, placental growth factor; TMB, tumour mutation burden; Treg, regulatory T cells; NK, natural killer; DC, dendritic cell.

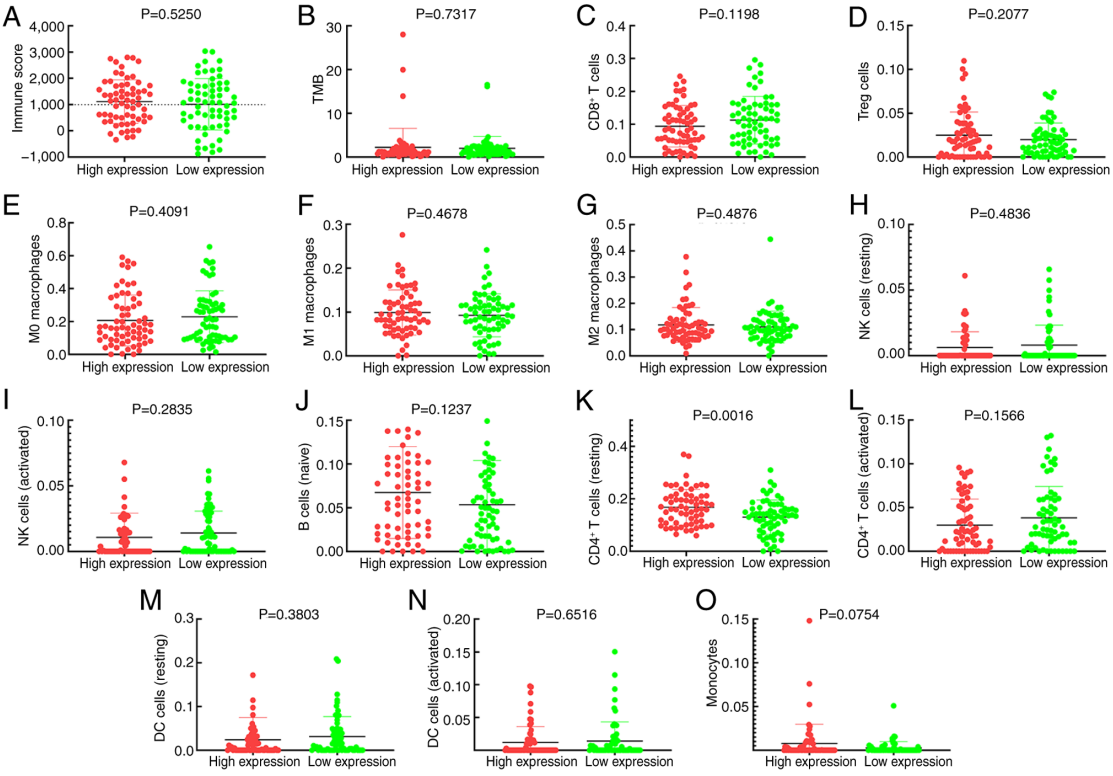

Figure 6. LTBP2 and immune cell infiltration association analysis by Mann-Whitney U test. Association of LTBP2 expression with (A) immune score, (B) TMB, (C) $CD8^+$ T cells, (D) Treg cells, (E) M0 macrophages, (F) M1 macrophages, (G) M2 macrophages, (H) NK cells (resting), (I) NK cells (activated), (J) B cells, (K) $CD4^+$ T cells (resting), (L) $CD4^+$ T cells (activated), (M) DC cells (resting), (N) DCs (activated) and (O) monocytes. LTBP2, latent TGF-β binding protein 2; TMB, tumour mutation burden; Treg, regulatory T cell; NK, natural killer; DC, dendritic cell.

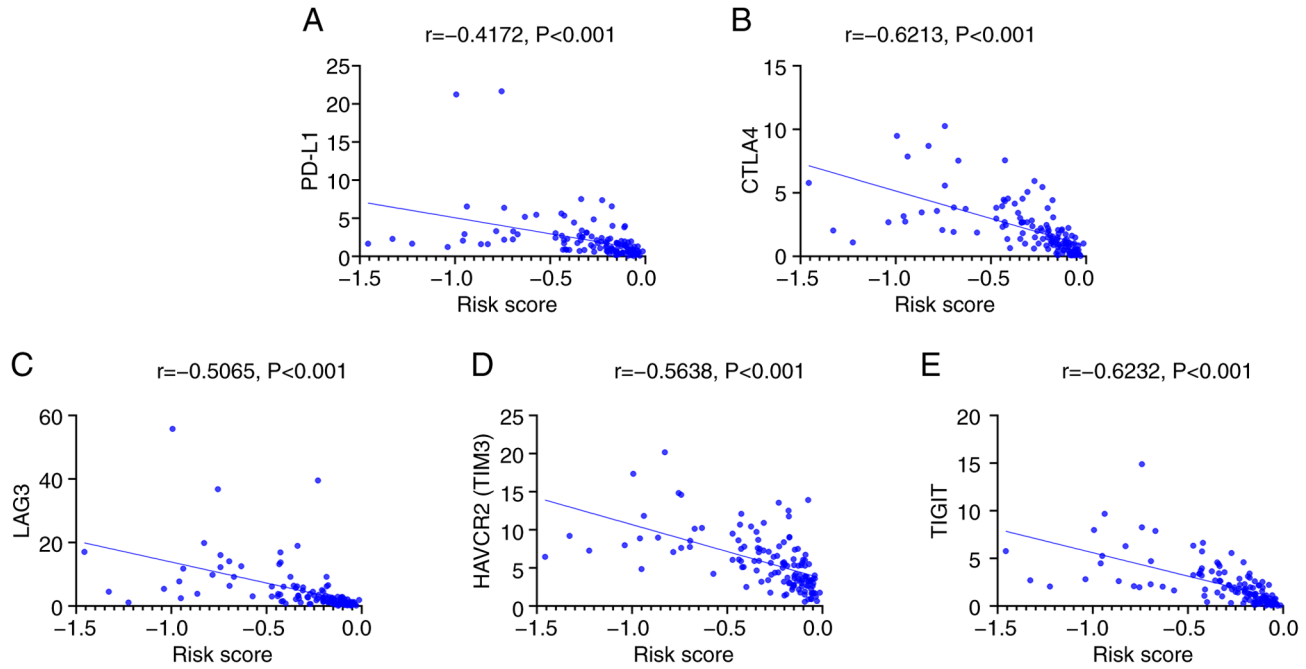

Figure 7. Risk score and immune checkpoint-related genes correlation analysis. Correlation between risk score and (A) PD-L1, (B) CTLA4, (C) LAG3, (D) TIM3 and (E) TIGIT. PD-L1, programmed cell death-ligand 1; CTLA4, cytotoxic T-lymphocyte antigen 4; TIM3, T-cell immunoglobulin and mucin domain-containing protein 3; LAG3, lymphocyte activation gene 3; TIGIT, T-cell immunoreceptor with Ig and immunoreceptor tyrosine-based inhibitory motif domains.

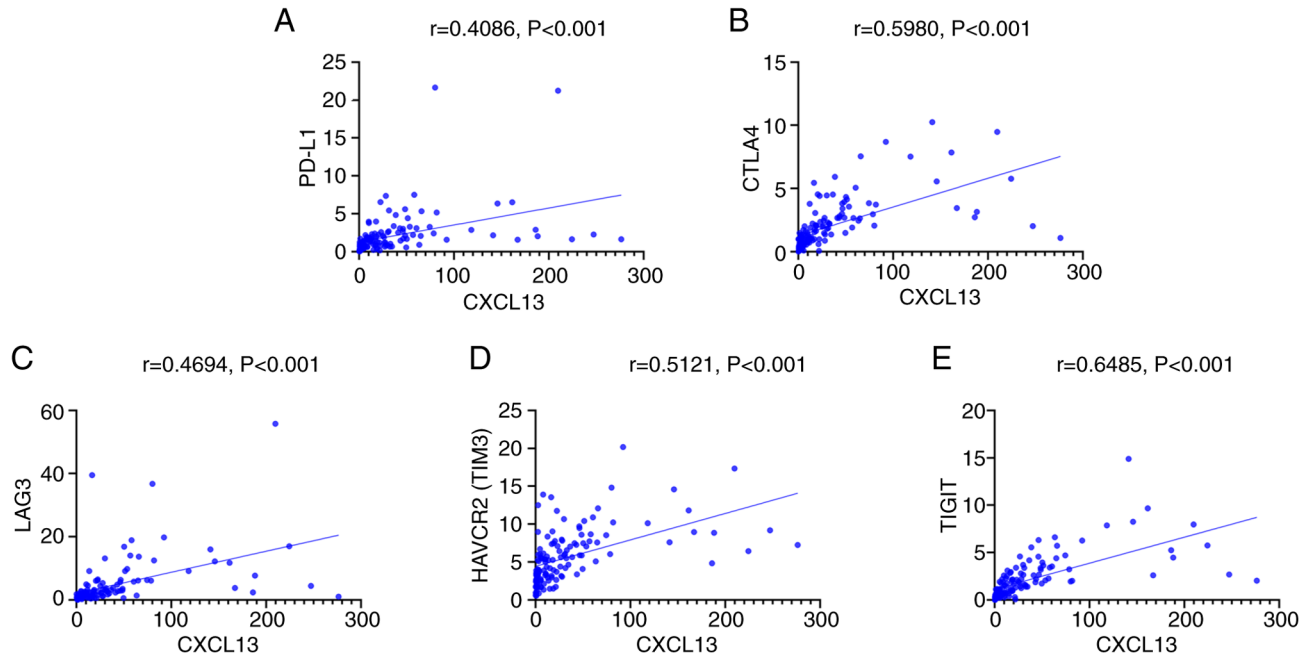

Figure 8. CXCL13 and immune checkpoint-related genes correlation analysis. Correlation between CXCL13 expression and (A) PD-L1, (B) CTLA4, (C) LAG3, (D) TIM3 and (E) TIGIT. CXCL13, C-X-C motif chemokine ligand 13; PD-L1, programmed cell death-ligand 1; CTLA4, cytotoxic T-lymphocyte antigen 4; TIM3, T-cell immunoglobulin and mucin domain-containing protein 3; LAG3, lymphocyte activation gene 3; TIGIT, T-cell immunoreceptor with Ig and immunoreceptor tyrosine-based inhibitory motif domains.

correlation was observed between PD-L1, TIM3, TIGIT, CTLA-4 and LTBP2 (Fig. 11).

TIDE score analysis of survival-associated IRGs. Individuals classified as low-risk had a markedly lower TIDE score compared with the high-risk group (Fig. 12A). Higher levels of CXCL13 expression were associated with lower TIDE scores (Fig. 12B). Similarly, individuals with higher levels of TAPBPL expression had lower TIDE scores compared with low levels of TAPBPL expression (Fig. 12C). By contrast, higher levels of PGF expression were associated with higher TIDE scores (Fig. 12D). There was no significant difference

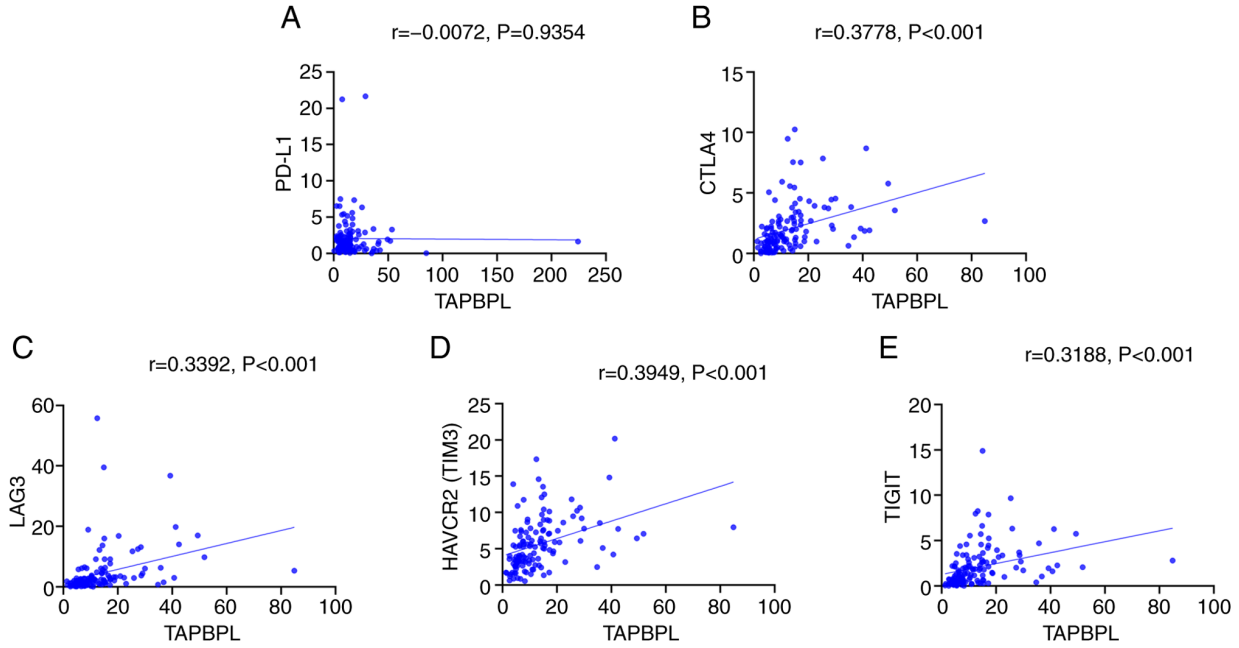

Figure 9. TAPBPL and immune checkpoint-related genes correlation analysis. Correlation between TAPBPL expression and (A) PD-L1, (B) CTLA4, (C) LAG3, (D) TIM3 and (E) TIGIT. TAPBPL, transporter associated with antigen processing binding protein like; PD-L1, programmed cell death-ligand 1; CTLA4, cytotoxic T-lymphocyte antigen 4; TIM3, T-cell immunoglobulin and mucin domain-containing protein 3; LAG3, lymphocyte activation gene 3; TIGIT, T-cell immunoreceptor with Ig and immunoreceptor tyrosine-based inhibitory motif domains.

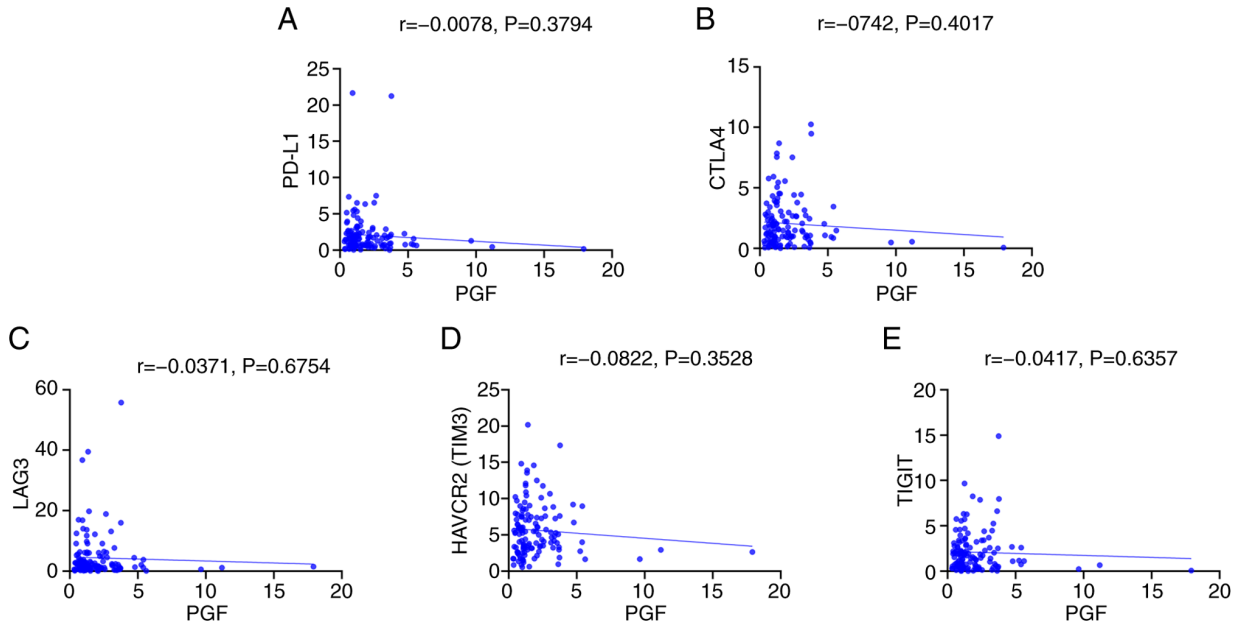

Figure 10. PGF and immune checkpoint-related genes correlation analysis. Correlation between PGF expression and (A) PD-L1, (B) CTLA4, (C) LAG3, (D) TIM3 and (E) TIGIT. PGF, placental growth factor; PD-L1, programmed cell death-ligand 1; CTLA4, cytotoxic T-lymphocyte antigen 4; TIM3, T-cell immunoglobulin and mucin domain-containing protein 3; LAG3, lymphocyte activation gene 3; TIGIT, T-cell immunoreceptor with Ig and immunoreceptor tyrosine-based inhibitory motif domains.

in the TIDE score between risk categories with LTBP2 expression (Fig. 12E).

Validation of survival-associated IRGs expression in TNBC tissues. To assess protein expression levels of CXCL13, TAPBPL, LTBP2 and PGF, IHC analysis was performed on TNBC samples. In support of the immune cell infiltrating data, TNBC tissues with high CD8 expression levels demonstrated strong CXCL13 and TAPBPL expression, while LTBP2 and PGF demonstrated weak IHC signals (Fig. S6).

Discussion

The host immune system demonstrates a well-established double-edged sword effect on neoplasia. Immune elements can

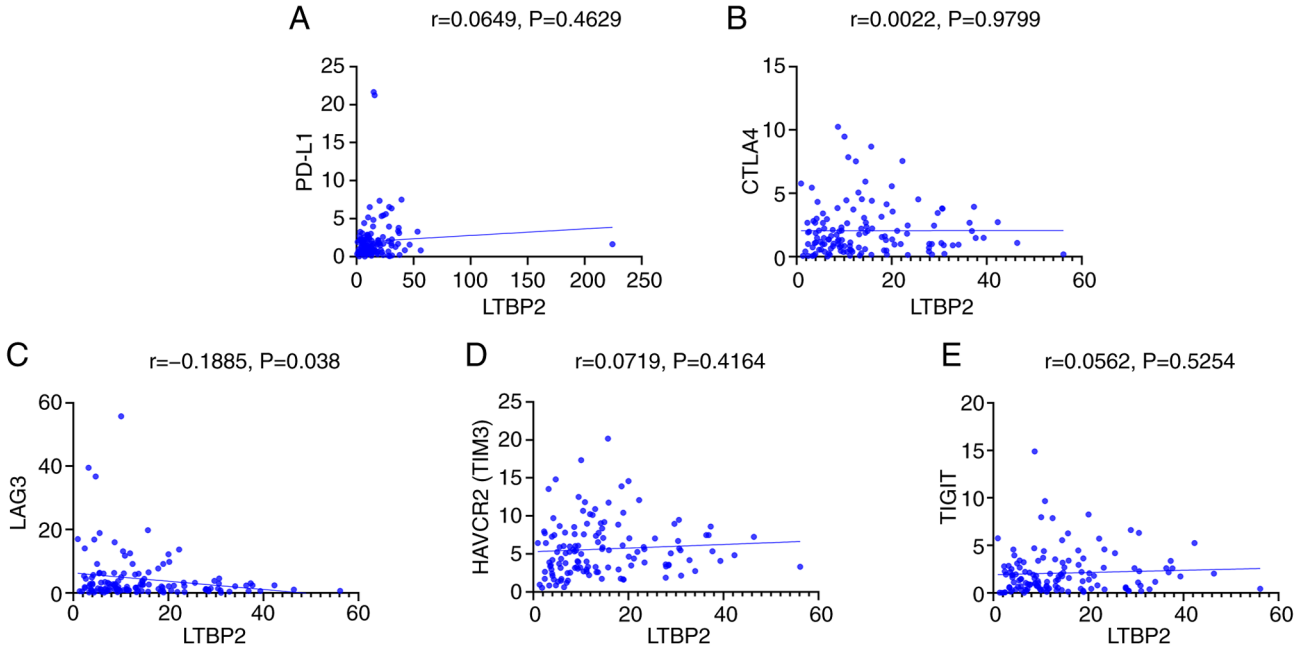

Figure 11. LTBP2 and immune checkpoint-related genes correlation analysis. Correlation between LTBP2 expression and (A) PD-L1, (B) CTLA4, (C) LAG3, (D) TIM3 and (E) TIGIT. LTBP2, latent TGF-β binding protein 2; PD-L1, programmed cell death-ligand 1; CTLA4, cytotoxic T-lymphocyte antigen 4; TIM3, T-cell immunoglobulin and mucin domain-containing protein 3; LAG3, lymphocyte activation gene 3; TIGIT, T-cell immunoreceptor with Ig and immunoreceptor tyrosine-based inhibitory motif domains.

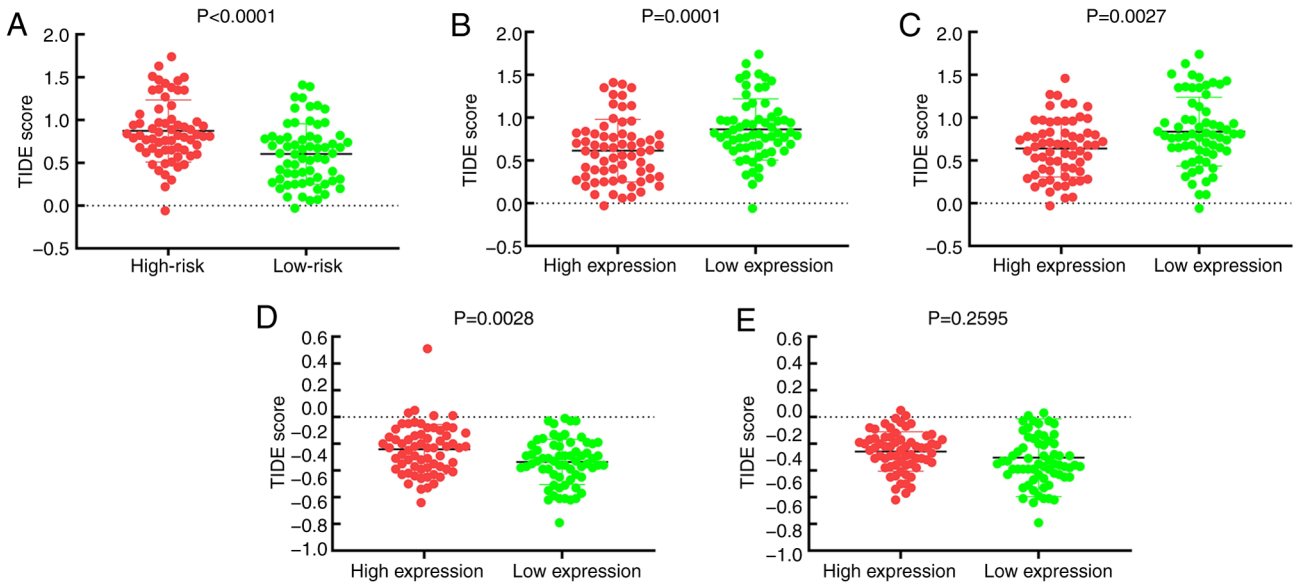

Figure 12. TIDE score analysis using a t-test. Association of TIDE score with (A) risk score and (B) CXCL13, (C) TAPBPL, (D) PGF and (E) LTBP2 expression. CXCL13, C-X-C motif chemokine ligand 13; TAPBPL, transporter associated with antigen processing binding protein like; PGF, placental growth factor; LTBP2, latent TGF-β binding protein 2; TIDE, tumour dysfunction and exclusion.

potentially drive malignancy yet provide strong antitumour and cytotoxic functions (38). Therefore, ICIs have become standard treatment for certain relapsed or metastatic diseases, such as TNBC. Clinical trials such as KEYNOTE-522 (NCT03036488) and IMpassion-130 (NCT02425891) led to the regulatory approval of pembrolizumab and atezolizumab for recurrent or metastatic TNBC (39-41); however, while there were notable clinical benefits in these studies, they were mostly confined to tumours with a high combined positive score (CPS). Since CPS-high lesions are a small subset of all breast cancer types, it is key to find novel predictive biomarkers to improve the precision and population-wide benefit of treatment in TNBC. Notable evidence has demonstrated that a high TMB is notably correlated with enhanced T-cell infiltration, higher neoantigen burden, improved response to ICIs and prolonged survival in TNBC (42,43). Considering the value of TMB and TILs in evaluating the efficacy of ICIs (44,45), the present study therefore focused on their prognostic value in TNBC.

In the present study, 130 patients with TNBC were assigned to $TMB^{high}/CD8^{+}$ T-$cell^{high}$ or $TMB^{low}/CD8^{+}$ T-$cell^{low}$ groups.

Kaplan-Meier analysis indicated that the $TMB^{high}/CD8^+$ $T\text{-}cell^{high}$ cohort had a significantly improved survival outcome compared with the $TMB^{low}/CD8^+$ $T\text{-}cell^{low}$ group. Higher TMB and $CD8^+$ T cell levels may create neo-antigens that enhance immune recognition, increase sensitivity to immune-checkpoint blockade and provide improved response rates and survival. Therefore, individuals with high TMB and $CD8^+$ expression have improved prognosis (46,47). Further investigation revealed 14 genes were differentially expressed, immune-related and had prognostic value. To corroborate these observations, external validation was performed using the GEO dataset GSE58812 to reduce the applicable genes to obtain a prognostic model based on five IRGs.

Subsequently, differential transcripts between defined risk strata were used to perform classification across these two groups to create a prognostic signature. Tumour immune microenvironment (TIME) characterisation revealed that low-risk tumours had a denser intratumoral $CD8^+$ T-cell infiltration with a higher global IS but richer M2-polarised macrophages in the high-risk tumours. Previous studies established that $CD8^+$ T effector cells are the predominant lymphocyte infiltrate in breast tumours (14,48). Furthermore, heightened T-cell infiltration is associated with objective response rates among patients with TNBC who receive ICI therapy (49) and the intratumoral vs. stromal compartment of $CD8^+$ T-lymphocytes is associated with enhanced relapse-free survival (50). By contrast, IL-6, IL-17 and TGF-β cytokines have demonstrated the ability to activate tumour-associated macrophages and Tregs to inhibit $CD8^+$ T cell proliferation, migration and cytolytic function by releasing immunosuppressive mediators (51-53). Macrophages themselves exhibit two main activation states: i) Classically activated (M1), providing antimicrobial defence; and ii) alternatively activated (M2), promoting metastases, an immunosuppressive environment and angiogenesis (54-57). Therefore, the accumulation of M1 macrophages and $CD8^+$ T cells from the low-risk cluster could explain their improved clinical course.

The present study identified four immune-related prognostic genes including CXCL13, TAPBPL, LTBP2 and PGF. CXCL13, also known as B-lymphocyte attracting chemokine 1, attracts CXC receptor 5^+ B cells and promotes germinal-centre activity (58). Several studies associate elevated CXCL13 levels with improved disease-free survival and higher pathologic complete response rates after neoadjuvant chemotherapy treatment in patients with TNBC (59,60). Lv *et al* (61) demonstrated that there was a greater chemotherapy response in patients with high expression of CXCL13 than those with low expression of CXCL13 in TNBCs. TAPBPL is expressed by resting and activated T cells, B cells, DCs and monocytes. Experimental investigations demonstrated that TAPBPL inhibits T cell activation *in vitro* and its inhibition enhances antitumour immunity in culture and mice (62). CXCL10 was recognised as a strong T cell chemoattractant and orchestrates migration, differentiation and activation of immune cells (63,64). Yi *et al* (65) demonstrated CXCL10 is a key regulatory immune molecule and prognostic factor for TNBC; Katsuta *et al* (66) identified high CXCL10 expression levels facilitated antitumour immunity and improved survival. Indoleamine 2,3-dioxygenase 1 (IDO1) mRNA is upregulated in several cancer types, inhibiting T-cell infiltration and limiting pharmacological approaches targeting IDO1 (67,68). In TNBC, high IDO1 transcription is associated with recurrence <5 years after chemotherapy administration (69). IFNG remains one of the original effector cytokines for antitumour immunity and one of the most continuously associated predictors for ICI candidate-responding tumours (70,71). Increased transcription of IFNG was reported to be strongly associated with improved disease-free survival in TNBC (HR=0.38) (72).

The present risk-score analysis indicated that high CXCL13 expression in TNBC samples is associated with significantly higher IS scores, increased overall $CD8^+$ T cells and increased M1 macrophages and significantly lower M2 macrophages, indicating a more pro-immunogenic antitumour immune environment. CXCL13 demonstrated strong positive correlations with multiple immune-checkpoint genes (PD-L1, TIM3, LAG3, CTLA-4 and TIGIT), indicating that CXCL13 reflects TIME state and predicts ICI response. Increased TAPBPL expression was also positively correlated with increased IS score and $CD8^+$ T-cell density and inversely correlated with increased M0 and M2 macrophages. Furthermore, increased TAPBPL expression demonstrated positive correlations with CTLA4, TIM3 and LAG3. PGF is a member of the vascular endothelial growth factor family that promotes neovascularisation and inflammation (72); here, increased PGF expression was significantly associated with greater infiltration of M0 and lower infiltration of M1 macrophages. LTBP2, which has been implicated in various malignancies (73), indicated significantly inverse correlations with LAG3. Due to the contrasting pro- and anti-differentiation functions of M1 and M2 macrophages in cancer biology, these IRGs might represent actionable biomarkers that could be used for treatment decisions and prognosis in TNBC.

Finally, to validate the accuracy of this prognostic model, we constructed ROC curves and a nomogram to compare the predictive efficacy across different ages, AJCC, T stages, N stages, and risk scores. In the ROC analysis, both the risk score and N stage yielded AUC values greater than 0.8, demonstrating excellent diagnostic performance. Meanwhile, the nomogram clearly indicates that a lower total score corresponds to higher 3, 5, and 10-year survival rates, which aligns with clinical expectations. In summary, compared with conventional methods, the present prognostic model exhibits superior predictive accuracy.

To further explore immune evasion mechanisms, the present study also calculated TIDE scores, with larger scores representing an increased propensity to immune escape and resistance to ICI therapy. Low-risk TNBC tumours and tumours with high CXCL13, TAPBPL or PGF expression demonstrated statistically lower TIDE scores, indicating these tumours might be more susceptible to checkpoint blockade.

To the best of our knowledge, the present study is the first to combine TMB status with $CD8^+$ T-cell infiltration in an overall immunogenomic context to produce an overall risk model of IRGs for TNBC. In addition, the present study demonstrated that the risk signature is closely associated multiple immune-checkpoint mediators, advancing the current understanding of the TNBC immune landscape and providing a potential biomarker for the prospective prediction of immunotherapy benefit in this aggressive subtype of breast cancer.

There are still certain limitations in the present study. Firstly, the prognostic index in the present study was based on gene expression data provided by TCGA, and the high price and long testing time might limit the application of the prognostic index in clinical practice. Secondly, despite the approval of ICIs for the first-line treatment of recurrent and metastatic TNBC, the number of patients receiving ICI treatment is currently limited. Thus, more cases undergoing ICI treatment are warranted in future investigations. Furthermore, due to the relatively low incidence rate of TNBC, the present study did not have sufficient samples to quantitatively analyse the association between the expression levels of PD-L1 and immune-related genes in the tumour immune microenvironment. Future studies may include a larger sample size to verify the present study findings.

Acknowledgements

Not applicable.

Funding

The present study was supported by Science and Technology Project Foundation of Suzhou (grant no. SKJY2021126) and Clinical Oncology Research Foundation of Beijing CSCO (grant no. Y-Young2021-0087).

Availability of data and materials

The data generated in the present study may be requested from the corresponding author.

Authors' contributions

WW, YW and YoM designed the present study. YW and YoM provided administrative support. WW, LL and JZ provided study materials and recruited patients. ZH, YinL, YH and ZZ collected the data. ZH, YuM, YifL and HW conducted the data analysis and interpretation. WW and YuM confirm the authenticity of all the data. All authors wrote the main manuscript. All authors read and approved the final manuscript.

Ethics approval and consent to participate

The research protocol was approved by the Ethics Committee of Suzhou Municipal Hospital (approval no. K-2022-019-K01; Suzhou, China) and conforms to the provisions of the Declaration of Helsinki. Written informed consent was provided by all patients prior to the surgical operation.

Patient consent for publication

Not applicable.

Competing interests

The authors declare that they have no competing interests.

References

1. Lei H, Fu J, Gu W, Qiao H, Guo H, Chen Z, Wang SM and Chen T: Breast cancer: Molecular pathogenesis, targeted therapy, screening, and prevention. MedComm (2020) 7: e70560, 2026.
2. Cancer Genome Atlas Network: Comprehensive molecular portraits of human breast tumours. Nature 490: 61-70, 2012.
3. Dent R, Trudeau M, Pritchard KI, Hanna WM, Kahn HK, Sawka CA, Lickley LA, Rawlinson E, Sun P and Narod SA: Triple-negative breast cancer: Clinical features and patterns of recurrence. Clin Cancer Res 13: 4429-4434, 2007.
4. Lehmann BD, Bauer JA, Chen X, Sanders ME, Chakravarthy AB, Shyr Y and Pietenpol JA: Identification of human triple-negative breast cancer subtypes and preclinical models for selection of targeted therapies. J Clin Invest 121: 2750-2767, 2011.
5. Palma M: Advancing breast cancer treatment: The role of immunotherapy and cancer vaccines in overcoming therapeutic challenges. Vaccines (Basel) 13: 344, 2025.
6. Lyons TG, Dickler MN and Comen EE: Checkpoint inhibitors in the treatment of breast cancer. Curr Oncol Rep 20: 51, 2018.
7. Ye J, Wu S, Quan Q, Ye F, Zhang J, Song C, Fan Y, Cao H, Tang H and Zhao J: Fibroblast growth factor receptor 4 promotes triple-negative breast cancer progression via regulating fatty acid metabolism through the AKT/RYR2 signaling. Cancer Med 13: e70439, 2024.
8. Xu A, Li X, Cai Q, Yang C, Yang M, Gao H, Cheng M, Chen X, Ji F, Tang H and Wang K: CircXPO6 promotes breast cancer progression through competitively inhibiting the ubiquitination degradation of c-Myc. Mol Cell Biochem 480: 1731-1745, 2025.
9. Emens LA: Breast cancer immunotherapy: Facts and hopes. Clin Cancer Res 24: 511-520, 2018.
10. Loi S: Tumor-infiltrating lymphocytes, breast cancer subtypes and therapeutic efficacy. Oncoimmunology 2: e24720, 2013.
11. Adams S, Gray RJ, Demaria S, Goldstein L, Perez EA, Shulman LN, Martino S, Wang M, Jones VE, Saphner TJ, *et al*: Prognostic value of tumor-infiltrating lymphocytes in triple-negative breast cancers from two phase III randomized adjuvant breast cancer trials: ECOG 2197 and ECOG 1199. J Clin Oncol 32: 2959-2966, 2014.
12. Dieci MV, Criscitiello C, Goubar A, Viale G, Conte P, Guarneri V, Ficarra G, Mathieu MC, Delaloge S, Curigliano G and Andre F: Prognostic value of tumor-infiltrating lymphocytes on residual disease after primary chemotherapy for triple-negative breast cancer: A retrospective multicenter study. Ann Oncol 25: 611-618, 2014.
13. Adams S, Goldstein LJ, Sparano JA, Demaria S and Badve SS: Tumor infiltrating lymphocytes (TILs) improve prognosis in patients with triple negative breast cancer (TNBC). Oncoimmunology 4: e985930, 2015.
14. Mahmoud SMA, Paish EC, Powe DG, Macmillan RD, Grainge MJ, Lee AH, Ellis IO and Green AR: Tumor-infiltrating CD8+ lymphocytes predict clinical outcome in breast cancer. J Clin Oncol 29: 1949-1955, 2011.
15. Taube JM, Klein A, Brahmer JR, Xu H, Pan X, Kim JH, Chen L, Pardoll DM, Topalian SL and Anders RA: Association of PD-1, PD-1 ligands, and other features of the tumor immune microenvironment with response to anti-PD-1 therapy. Clin Cancer Res 20: 5064-5074, 2014.
16. Tumeh PC, Harview CL, Yearley JH, Shintaku IP, Taylor EJ, Robert L, Chmielowski B, Spasic M, Henry G, Ciobanu V, *et al*: PD-1 blockade induces responses by inhibiting adaptive immune resistance. Nature 515: 568-571, 2014.
17. Liu L, Bai X, Wang J, Tang XR, Wu DH, Du SS, Du XJ, Zhang YW, Zhu HB, Fang Y, *et al*: Combination of TMB and CNA stratifies prognostic and predictive responses to immunotherapy across metastatic cancer. Clin Cancer Res 25: 7413-7423, 2019.
18. Brown SD, Warren RL, Gibb EA, Martin SD, Spinelli JJ, Nelson BH and Holt RA: Neo-antigens predicted by tumor genome meta-analysis correlate with increased patient survival. Genome Res 24: 743-750, 2014.
19. Kumari N, Dwarakanath BS, Das A and Bhatt AN: Role of interleukin-6 in cancer progression and therapeutic resistance. Tumour Biol 37: 11553-11572, 2016.
20. Warburg O: On the origin of cancer cells. Science 123: 309-314, 1956.
21. Chalmers ZR, Connelly CF, Fabrizio D, Gay L, Ali SM, Ennis R, Schrock A, Campbell B, Shlien A, Chmielecki J, *et al*: Analysis of 100,000 human cancer genomes reveals the landscape of tumor mutational burden. Genome Med 9: 34, 2017.

22. Samstein RM, Lee CH, Shoushtari AN, Hellmann MD, Shen R, Janjigian YY, Barron DA, Zehir A, Jordan EJ, Omuro A, *et al*: Tumor mutational load predicts survival after immunotherapy across multiple cancer types. Nat Genet 51: 202-206, 2019.
23. Rody A, Holtrich U, Pusztai L, Liedtke C, Gaetje R, Ruckhaeberle E, Solbach C, Hanker L, Ahr A, Metzler D, *et al*: T-cell metagene predicts a favorable prognosis in estrogen receptor-negative and HER2-positive breast cancers. Breast Cancer Res 11: R15, 2009.
24. Iglesia MD, Parker JS, Hoadley KA, Serody JS, Perou CM and Vincent BG: Genomic analysis of immune cell infiltrates across 11 tumor types. J Natl Cancer Inst 108: djw144, 2016.
25. Bedognetti D, Hendrickx W, Marincola FM and Miller LD: Prognostic and predictive immune gene signatures in breast cancer. Curr Opin Oncol 27: 433-444, 2015.
26. Liu Y, Hu Y, Xue J, Li J, Yi J, Bu J, Zhang Z, Qiu P and Gu X: Advances in immunotherapy for triple-negative breast cancer. Mol Cancer 22: 145, 2023.
27. Villacampa G, Navarro V, Matikas A, Ribeiro JM, Schettini F, Tolosa P, Martínez-Sáez O, Sánchez-Bayona R, Ferrero-Cafiero JM, Salvador F, *et al*: Neoadjuvant immune checkpoint inhibitors plus chemotherapy in early breast cancer: A systematic review and meta-analysis. JAMA Oncol 10:1331-1341, 2024.
28. Das R, Deb S and Suresh PK: TMB as a predictive biomarker for ICI response in TNBC: Current evidence and future directions for augmented anti-tumor responses. Clin Exp Med 26: 25, 2025.
29. Wang X and Chen H: Prognosis prediction through an integrated analysis of single-cell and bulk RNA-sequencing data in triple-negative breast cancer. Front Genet 13: 928175, 2022.
30. Thomas A, Routh ED, Pullikuth A, Jin G, Su J, Chou JW, Hoadley KA, Print C, Knowlton N, Black MA, *et al*: Tumor mutational burden is a determinant of immune-mediated survival in breast cancer. Oncoimmunology 7: e1490854, 2018.
31. Bhattacharya S, Andorf S, Gomes L, Dunn P, Schaefer H, Pontius J, Berger P, Desborough V, Smith T, Campbell J, *et al*: ImmPort: Disseminating data to the public for the future of immunology. Immunol Res 58: 234-239, 2014.
32. Jézéquel P, Loussouarn D, Guérin-Charbonnel C, Campion L, Vanier A, Gouraud W, Lasla H, Guette C, Valo I, Verrièle V and Campone M: Gene-expression molecular subtyping of triple-negative breast cancer tumours: Importance of immune response. Breast Cancer Res 17: 43, 2015.
33. Robinson MD, McCarthy DJ and Smyth GK: edgeR: A bioconductor package for differential expression analysis of digital gene expression data. Bioinformatics 26: 139-140, 2010.
34. Liu J, Lichtenberg T, Hoadley KA, Poisson LM, Lazar AJ, Cherniack AD, Kovatich AJ, Benz CC, Levine DA, Lee AV, *et al*: An integrated TCGA pan-cancer clinical data resource to drive high-quality survival outcome analytics. Cell 173: 400-416.e11, 2018.
35. Li T, Fan J, Wang B, Traugh N, Chen Q, Liu JS, Li B and Liu XS: TIMER: A web server for comprehensive analysis of tumor-infiltrating immune cells. Cancer Res 77: e108-e110, 2017.
36. Giuliano AE, Connolly JL, Edge SB, Mittendorf EA, Rugo HS, Solin LJ, Weaver DL, Winchester DJ and Hortobagyi GN: Breast cancer-major changes in the American joint committee on cancer eighth edition cancer staging manual. CA Cancer J Clin 67: 290-303, 2017.
37. McCarty KS Jr, Szabo E, Flowers JL, Cox EB, Leight GS, Miller L, Konrath J, Soper JT, Budwit DA, Creasman WT, *et al*: Use of a monoclonal anti-estrogen receptor antibody in the immunohistochemical evaluation of human tumors. Cancer Res 46 (8 Suppl): 4244s-4248s, 1986.
38. Vikas P, Borcherding N and Zhang W: The clinical promise of immunotherapy in triple-negative breast cancer. Cancer Manag Res 10: 6823-6833, 2018.
39. Halama A, Takada K, Takamori S, Haratake N, Akamine T, Kinoshita F, Ono Y, Wakasu S, Tanaka K, Oku Y, *et al*: Clinical significance of preoperative inflammatory markers in non-small cell lung cancer patients: A multicenter retrospective study. PLoS One 15: e0241580, 2020.
40. Dent R, Cortés J, Pusztai L, McArthur H, Kümmel S, Bergh J, Denkert C, Park YH, Hui R, Harbeck N, *et al*: Neoadjuvant pembrolizumab plus chemotherapy/adjuvant pembrolizumab for early-stage triple-negative breast cancer: Quality-of-life results from the randomized KEYNOTE-522 study. J Natl Cancer Inst 116: 1654-1663, 2024.
41. Schmid P, Rugo HS, Adams S, Schneeweiss A, Barrios CH, Iwata H, Diéras V, Henschel V, Molinero L, Chui SY, *et al*: Atezolizumab plus nab-paclitaxel as first-line treatment for unresectable, locally advanced or metastatic triple-negative breast cancer (IMpassion130): Updated efficacy results from a randomised, double-blind, placebo-controlled, phase 3 trial. Lancet Oncol 21: 44-59, 2020.
42. Sukumar J, Gast K, Quiroga D, Lustberg M and Williams N: Triple-negative breast cancer: promising prognostic biomarkers currently in development. Expert Rev Anticancer Ther 21: 135-148, 2021.
43. Dvir K, Giordano S and Leone JP: Immunotherapy in breast cancer. Int J Mol Sci 25: 7517, 2024.
44. Ravelli A, Roviello G, Cretella D, Cavazzoni A, Biondi A, Cappelletti MR, Zanotti L, Ferrero G, Ungari M, Zanconati F, *et al*: Tumor-infiltrating lymphocytes and breast cancer: Beyond the prognostic and predictive utility. Tumour Biol 39: 1010428317695023, 2017.
45. Dushyanthen S, Beavis PA, Savas P, Teo ZL, Zhou C, Mansour M, Darcy PK and Loi S: Relevance of tumor-infiltrating lymphocytes in breast cancer. BMC Med 13: 202, 2015.
46. Rizvi NA, Hellmann MD, Snyder A, Kvistborg P, Makarov V, Havel JJ, Lee W, Yuan J, Wong P, Ho TS, *et al*: Cancer immunology. Mutational landscape determines sensitivity to PD-1 blockade in non-small cell lung cancer. Science 348: 124-128, 2015.
47. Naing A, Infante JR, Papadopoulos KP, Chan IH, Shen C, Ratti NP, Rojo B, Autio KA, Wong DJ, Patel MR, *et al*: PEGylated IL-10 (Pegilodecakin) induces systemic immune activation, $CD8^+$ T cell invigoration and polyclonal T cell expansion in cancer patients. Cancer Cell 34: 775-791.e3, 2018.
48. Bense RD, Sotiriou C, Piccart-Gebhart MJ, Haanen JBAG, van Vugt MATM, de Vries EGE, Schröder CP and Fehrmann RSN: Relevance of tumor-infiltrating immune cell composition and functionality for disease outcome in breast cancer. J Natl Cancer Inst 109: djw192, 2016.
49. Zou Y, Zou X, Zheng S, Tang H, Zhang L, Liu P and Xie X: Efficacy and predictive factors of immune checkpoint inhibitors in metastatic breast cancer: A systematic review and meta-analysis. Ther Adv Med Oncol 12: 1758835920940928, 2020.
50. Egelston CA, Avalos C, Tu TY, Rosario A, Wang R, Solomon S, Srinivasan G, Nelson MS, Huang Y, Lim MH, *et al*: Resident memory CD8+ T cells within cancer islands mediate survival in breast cancer patients. JCI Insight 4: e130000, 2019.
51. Gatti-Mays ME, Balko JM, Gameiro SR, Bear HD, Prabhakaran S, Fukui J, Disis ML, Nanda R, Gulley JL, Kalinsky K, *et al*: If we build it they will come: Targeting the immune response to breast cancer. NPJ Breast Cancer 5: 37, 2019.
52. Doedens AL, Stockmann C, Rubinstein MP, Liao D, Zhang N, DeNardo DG, Coussens LM, Karin M, Goldrath AW and Johnson RS: Macrophage expression of hypoxia-inducible factor-1 alpha suppresses T-cell function and promotes tumor progression. Cancer Res 70: 7465-7475, 2010.
53. Ruffell B, Chang-Strachan D, Chan V, Rosenbusch A, Ho CM, Pryer N, Daniel D, Hwang ES, Rugo HS and Coussens LM: Macrophage IL-10 blocks CD8+ T cell-dependent responses to chemotherapy by suppressing IL-12 expression in intratumoral dendritic cells. Cancer Cell 26: 623-637, 2014.
54. Montes VN, Turner MS, Subramanian S, Ding Y, Hayden-Ledbetter M, Slater S, Goodspeed L, Wang S, Omer M, Den Hartigh LJ, *et al*: T cell activation inhibitors reduce CD8+ T cell and pro-inflammatory macrophage accumulation in adipose tissue of obese mice. PLoS One 8: e67709, 2013.
55. Xu Y, Romero R, Miller D, Kadam L, Mial TN, Plazyo O, Garcia-Flores V, Hassan SS, Xu Z, Tarca AL, *et al*: An M1-like macrophage polarization in decidual tissue during spontaneous preterm labor that is attenuated by rosiglitazone treatment. J Immunol 196: 2476-2491, 2016.
56. Mao Y, Keller ET, Garfield DH, Shen K and Wang J: Stromal cells in tumor microenvironment and breast cancer. Cancer Metastasis Rev 32: 303-315, 2013.
57. Qian BZ and Pollard JW: Macrophage diversity enhances tumor progression and metastasis. Cell 141: 39-51, 2010.
58. Daou HN: Exercise as an anti-inflammatory therapy for cancer cachexia: A focus on interleukin-6 regulation. Am J Physiol Regul Integr Comp Physiol 318: R296-R310, 2020.
59. Denkert C, Loibl S, Noske A, Roller M, Müller BM, Komor M, Budczies J, Darb-Esfahani S, Kronenwett R, Hanusch C, *et al*: Tumor-associated lymphocytes as an independent predictor of response to neoadjuvant chemotherapy in breast cancer. J Clin Oncol 28: 105-113, 2010.

60. Lee HJ, Lee JJ, Song IH, Park IA, Kang J, Yu JH, Ahn JH and Gong G: Prognostic and predictive value of NanoString-based immune-related gene signatures in a neoadjuvant setting of triple-negative breast cancer: Relationship to tumor-infiltrating lymphocytes. Breast Cancer Res Treat 151: 619-627, 2015.
61. Lv Y, Lv D, Lv X, Xing P, Zhang J and Zhang Y: Immune cell infiltration-based characterization of triple-negative breast cancer predicts prognosis and chemotherapy response markers. Front Genet 12: 616469, 2021.
62. Lin Y, Cui C, Su M, Silbart LK, Liu H, Zhao J, He L, Huang Y, Xu D, Wei X, *et al*: Identification of TAPBPL as a novel negative regulator of T-cell function. EMBO Mol Med 13: e13404, 2021.
63. Yu Y, Li J, Zhu X, Tang X, Bao Y, Sun X, Huang Y, Tian F, Liu X and Yang L: Humanized CD7 nanobody-based immunotoxins exhibit promising anti-T-cell acute lymphoblastic leukemia potential. Int J Nanomedicine 12: 1969-1983, 2017.
64. Tokunaga R, Zhang W, Naseem M, Puccini A, Berger MD, Soni S, McSkane M, Baba H and Lenz HJ: CXCL9, CXCL10, CXCL11/CXCR3 axis for immune activation-a target for novel cancer therapy. Cancer Treat Rev 63: 40-47, 2018.
65. Yi J, Shuang Z, Zhong W, Wu H, Feng J, Zouxu X, Huang X, Li S and Wang X: Identification of immune-related risk characteristics and prognostic value of immunophenotyping in TNBC. Front Genet 12: 730442, 2021.
66. Katsuta E, Yan L, Opyrchal M, Kalinski P and Takabe K: Cytotoxic T-lymphocyte infiltration and chemokine predict long-term patient survival independently of tumor mutational burden in triple-negative breast cancer. Ther Adv Med Oncol 13: 17588359211006680, 2021.
67. Li F, Zhang R, Li S and Liu J: IDO1: An important immunotherapy target in cancer treatment. Int Immunopharmacol 47: 70-77, 2017.
68. Cheong JE and Sun L: Targeting the IDO1/TDO2-KYN-AhR pathway for cancer immunotherapy-challenges and opportunities. Trends Pharmacol Sci 39: 307-325, 2018.
69. Pérez-Pena J, Tibor Fekete J, Páez R, Baliu-Piqué M, García-Saenz JÁ, García-Barberán V, Manzano A, Pérez-Segura P, Esparis-Ogando A, Pandiella A, *et al*: A Transcriptomic immunologic signature predicts favorable outcome in neoadjuvant chemotherapy treated triple negative breast tumors. Front Immunol 10: 2802, 2019.
70. Castro F, Cardoso AP, Gonçalves RM, Serre K and Oliveira MJ: Interferon-gamma at the crossroads of tumor immune surveillance or evasion. Front Immunol 9: 847, 2018.
71. Burke JD and Young HA: IFN-γ: A cytokine at the right time, is in the right place. Semin Immunol 43: 101280, 2019.
72. Yeong J, Lim JCT, Lee B, Li H, Ong CCH, Thike AA, Yeap WH, Yang Y, Lim AYH, Tay TKY, *et al*: Prognostic value of CD8 + PD-1+ immune infiltrates and PDCD1 gene expression in triple negative breast cancer. J Immunother Cancer 7: 34, 2019.
73. Chen J, Gao G, Wang H, Ye X, Zhou J and Lin J: Expression and clinical significance of latent-transforming growth factor beta-binding protein 2 in primary hepatocellular carcinoma. Medicine (Baltimore) 98: e17216, 2019.